Semiclassical analysis of extended dynamical mean-field equations

Sergey Pankov, Gabriel Kotliar, and Yukitoshi Motome*
Center for Materials Theory, Department of Physics and Astronomy, Rutgers University, Piscataway, New Jersey 08854
(Received 11 December 2001; revised manuscript received 13 May 2002; published 31 July 2002)

The extended dynamical mean field equations are analyzed using semiclassical methods for a model describing an interacting Fermi-Bose system. We compare the semiclassical approach with the exact quantum Monte Carlo method. We found the transition to an ordered state to be of the first order for any dimension below four.

DOI: 10.1103/PhysRevB.66.045117 PACS number(s): 71.38.−k, 64.60.Cn, 63.20.Dj, 63.20.Kr

I. INTRODUCTION

The dynamical mean field theory (DMFT), a recently developed many-body approach to strongly correlated electron systems, has been very successful in unraveling nonperturbative problems such as the Mott metal-to-insulator transition.[1] In spite of its many successes, this technique has several limitations resulting from its single-site character and from the lack of feedback of the nonlocal collective excitations on the one-particle spectra. Several approaches are being pursued to extend the scope of the DMFT method. In this paper we explore an extension of the DMFT method, the extended DMFT theory (EDMFT),[2,3,4] which maintains a local self-energy while incorporating feedback effects of the charge and spin dynamics in the one-electron properties. This method gives rise to quantum impurity problems with fermionic and bosonic baths that need to be solved self-consistently. This method has already been applied to wide class of models, such as the spin fermion model,[5] fermions interacting with long range (Coulomb) electron-electron interaction,[6] electron-phonon systems,[7] and frustrated magnets.[8]

The EDMFT equations are more involved than the conventional DMFT equations because they involve a solution of a self-consistency problem in an additional bosonic sector and only recently was a full numerical analysis of the self-consistency conditions of EDMFT carried out.[7] The interpretation of the EDMFT instabilities is also not as straightforward as in DMFT because bosonic and fermionic propagators involve very different regions of momentum space, and a formulation of EDMFT for ordered phases was only obtained recently.[9]

The purpose of this paper is to develop the EDMFT approach further by analyzing several aspects of this method. (i) We implement a semiclassical technique for its solution[10–12] and compare its results to the earlier quantum Monte Carlo (QMC) study[7] to test its accuracy. We show that the analytic treatment is in satisfactory agreement with exact (QMC) results in the high temperature regime of the three dimensional (3d) model and provides analytic expressions for various physical quantities. (ii) We extend this study to the case of two-dimensional (2d) phonons, which had not been treated in Ref. 7. We demonstrate that in the 2d case the EDMFT treatment at finite temperatures, if it produces an ordering transition, is necessarily of the first order. This analysis applies to a very general class of models including those used in Ref. 5.

We also analyze the EDMFT equations in the ordered phase,[9] for a simple spin model. This analysis clarifies the strengths and the limitations of the EDMFT approach, in a very simple setting.

The paper is organized as follows. In Sec. II we write the fermion boson model and the extended DMFT equations. Then we describe the semiclassical strategy for their analysis in both weak and strong electron-phonon coupling. In Sec. III we present results of solving the saddle-point equations for 3d phonons coupled to electrons in different regimes and discuss the agreement with results in the QMC approach. In Sec. IV we describe the results for 2d phonons. If the electrons are fully integrated out, the semiclassical treatment of EDMFT has to reduce to a mean-field theory in classical statistical mechanics. In Sec. V we compare EDMFT with other classical mean-field treatments such as the Weiss mean-field approach and the Bloch-Langer method.[13] The stability analysis of the EDMFT is carried out in Appendix D.

II. MODEL AND SEMICLASSICAL APPROXIMATION

The model under consideration is described by the lattice Hamiltonian

$$H = H_{el} + H_{ph} + H_{el\text{-}ph}, \tag{1}$$

where

$$H_{el} = -\sum_{ij,\sigma} t_{ij} c^{\dagger}_{i\sigma} c_{j\sigma}, \tag{2}$$

$$H_{ph} = \sum_{i} \frac{p_i^2}{2M} - \sum_{ij} \frac{J_{ij}}{2} x_i x_j, \tag{3}$$

$$H_{el\text{-}ph} = \sum_{i\sigma} \lambda x_i \left(c^{\dagger}_{i\sigma} c_{i\sigma} - \frac{1}{2} \right). \tag{4}$$

The first term describes free electrons, and $c^{\dagger}_{i\sigma}$ ($c_{i\sigma}$) creates (annihilates) an electron with spin σ on a site i. The second term describes nonlocal (dispersive) phonons, and x_i and p_i are canonical variables. The last term couples the fermionic and the bosonic degrees of freedom. We consider a half filled system of fermions.

The second term could alternatively be written as

$$H_{ph}=\sum_q \omega_q(a_q^\dagger a_q+\tfrac{1}{2}), \tag{5}$$

where a_q, $a_q^\dagger$ are related to the phonon field by $x_q=(2M\omega_q)^{-1/2}(a_q+a_{-q}^\dagger)$ and $\omega_q^2=J_q/M$. Dispersion (momentum dependence) of the boson frequency ω_q stems from the nonlocal character of J_{ij}. The local limit of J_{ij} corresponds to the Holstein model,[14] so the model under consideration is an extension of the Holstein model to dispersive phonons.

The extended DMFT equations for this model[7] are a set of equations for Weiss functions $G_{0\sigma}^{-1}(i\omega_n)$ and $D_0^{-1}(i\omega_n)$:

$$G_\sigma[G_0,D_0](i\omega_n)=\sum_q [i\omega_n-t_q+G_\sigma[G_0,D_0]^{-1}(i\omega_n) - G_{0\sigma}^{-1}(i\omega_n)]^{-1}, \tag{6}$$

$$D[G_0,D_0](i\omega_n)=\sum_q [M(i\omega_n)^2-J_q + D[G_0,D_0]^{-1}(i\omega_n)-D_0^{-1}(i\omega_n)]^{-1}, \tag{7}$$

where full Green's functions $G_\sigma(i\omega_n)$ and $D(i\omega_n)$ are expressed through $G_{0\sigma}^{-1}(i\omega_n)$ and $D_0^{-1}(i\omega_n)$ in terms of the effective impurity action:

$$S_{eff}=\sum_{\omega_n,\omega_m,\sigma} c_\sigma^\dagger(i\omega_n+i\omega_m)(G_{0\sigma}^{-1}(i\omega_n)\delta_{0,\omega_m} + \lambda x(i\omega_m))c_\sigma(i\omega_n)-\frac{1}{2}D_0^{-1}(i\omega_m)x^2(i\omega_m), \tag{8}$$

$$G_\sigma(i\omega_n)=\frac{\int \mathcal{D}[c_\sigma^\dagger,c_\sigma,x]c_\sigma(i\omega_n)c_\sigma^\dagger(i\omega_n)e^{-S_{eff}[c_\sigma^\dagger,c_\sigma,x]}}{\int \mathcal{D}[c_\sigma^\dagger,c_\sigma,x]e^{-S_{eff}[c_\sigma^\dagger,c_\sigma,x]}} =\langle c_\sigma(i\omega_n)c_\sigma^\dagger(i\omega_n)\rangle_{S_{eff}}, \tag{9}$$

$$D_\sigma(i\omega_n)=-\langle x^2(i\omega_n)\rangle_{S_{eff}}. \tag{10}$$

Equations (6)–(10) in general have to be solved numerically. In many cases though, a number of approximations reducing numerical work but preserving a physical content of the problem is possible. One of the approximations is in using a model density of states (DOS) for fermions and bosons, so that momentum summations in EDMFT equations could be performed analytically. It is convenient to chose a semicircular electron DOS,

$$\rho_{el}(\epsilon)=\frac{2}{\pi W^2}\sqrt{W^2-\epsilon^2}, \tag{11}$$

where W is the electron band half width. The particular choice of semicircular electron DOS is qualitatively unimportant since we consider a half filled electron band. For phonons, on the contrary, the shape of the phonon band near the bottom is crucial for temperatures smaller than the phonon bandwidth. For d-dimensional phonons the bottom of the band has $\epsilon^{(d-2)/2}$ singularity. That is why to represent 3d and 2d phonons we chose semicircular and step-function-like phonon densities of states, respectively:

$$3d: \quad \rho_{ph}(\epsilon)=\frac{2}{\pi\omega_1^2}\sqrt{\omega_1^2-(\epsilon-\omega_0)^2}, \tag{12}$$

$$2d: \quad \rho_{ph}(\epsilon)=\frac{1}{2\omega_1}\theta(\omega_1^2-(\epsilon-\omega_0)^2). \tag{13}$$

After replacing summations over wave vector by integrations over energy, Eq. (6) and Eq. (7) read

$$G_\sigma(i\omega_n)=\int d\epsilon\frac{\rho_{el}(\epsilon)}{\zeta-\epsilon}, \tag{14}$$

$$D(i\omega_n)=\int d\epsilon\frac{\rho_{ph}(\epsilon)}{\xi^2-\epsilon^2}, \tag{15}$$

where $\zeta=i\omega_n+G_\sigma^{-1}(i\omega_n)-G_{0\sigma}^{-1}(i\omega_n)$, $\xi^2=M(i\omega_n)^2+D^{-1}(i\omega_n)-D_0^{-1}(i\omega_n)$, and the density of states $\rho(\epsilon)\equiv dq/d\epsilon_q$. For electron $\rho_{el}(\epsilon)$ and phonon $\rho_{ph}(\epsilon)$ the densities of states are, respectively, $\epsilon_q=t_q$ and $\epsilon_q^2=J_q$. For the DOS defined in Eqs. (11)–(13) integrations over energy in Eqs. (14) and (15) yield

$$G_\sigma(i\omega_n)=\frac{2}{W^2}(\zeta-s\sqrt{\zeta^2-W^2}), \tag{16}$$

where $s=\mathrm{sgn}[\mathrm{Im}\zeta]$:

$$3d: \quad D(i\omega_n)=\frac{1}{\xi\omega_1^2}(2\xi+\sqrt{(\xi-\omega_0)^2-\omega_1^2} - \sqrt{(\xi+\omega_0)^2-\omega_1^2}), \tag{17}$$

$$2d: \quad D(i\omega_n)=\frac{1}{4\xi\omega_1}\ln\left[\frac{(\xi+\omega_1)^2-\omega_0^2}{(\xi-\omega_1)^2-\omega_0^2}\right]. \tag{18}$$

We consider here a semiclassical treatment of the problem. In its most general form, the approach has been described in Ref. 10 and is an application of the saddle-point method. In this paper we use a more limited form of this method that consists of evaluating Eqs. (9) and (10) by a saddle-point technique. It can be viewed as a combination of two separate approximations: the static approximation (equivalent to the phonon mass $M\to\infty$ limit) and a saddle-point analysis of the EDMFT equations in the static approximation.

The approach of treating the collective excitations as classical, while the electrons are treated fully quantum mechanically, goes back to the Hubbard approximation.[15] It was pointed out that a static approximation of the impurity model coupled with the DMFT self-consistency conditions indeed gives a solution closely related to Hubbard's.[16] This ap-

proach has been used extensively in Refs. 11 and 12 in DMFT studies of the Holstein model. From the DMFT studies of the Mott transition,[1] we know that this approach becomes insufficient in the correlated metallic regime at very low temperatures, where a quasiparticle feature forms in addition to the spectral features produced in the semiclassical approximation. It is worth pointing out that improvements of the static or of the saddle-point approximation,[10] will not remedy this shortcoming, which requires a nonperturbative resummation of instanton events. Still, we show here that this simple analysis is able to reproduce all the trends of the solution of the EDMFT equations by the more expensive QMC method.[7]

The EDMFT equations in the static approximation of Eqs. (9) and (10) reduce to

$$G(i\omega_n)=\int dxP(x)\frac{1}{G_0^{-1}(i\omega_n)+\lambda x}, \tag{19}$$

$$D=-\beta\int dxP(x)x^2, \tag{20}$$

where

$$P(x)=\frac{1}{N}\exp\left(g\sum_{n\geqslant 0}\ln(1-G_0(i\omega_n)^2\lambda^2x^2)-\frac{\beta}{2}D_0^{-1}x^2\right). \tag{21}$$

Equations (19)–(21) have to be solved together with Eqs. (6) and (7). In the static limit only the zero-phonon frequency survives, so we drop the frequency index for the phonon correlation functions D_0 and D. In Eqs. (19)–(21) and everywhere below we consider x being the phonon field amplitude, it is related to its Fourier transform as $x=\beta^{-1/2}x_{\omega_m=0}$. We consider no symmetry breaking in the electron-spin channel, so we dropped the spin index; factor g (equals 2 for spin one-half) in Eq. (21) appears from trace over the spin index. N normalizes $P(x)$ to unity. $P(x)$ is the probability distribution function of the phonon field amplitude x.

We now evaluate Eqs. (19)–(21) in the saddle-point approximation in the variable x. There are two limits, weak and strong coupling. In the weak coupling the saddle-point is at $x=0$, and in the strong coupling there are two equivalent saddle-points at $x=\pm x_0\neq 0$. Deriving the saddle-point equations we explicitly use a semicircular electron DOS, Eqs. (11) and (16). The relation between the bare and full Green's functions is especially simple in this case:

$$G_0(i\omega_n)^{-1}=i\omega_n-t^2G(i\omega_n), \tag{22}$$

where $t=W/2$. Everywhere below in this paper, energy is measured in units of t. In this paper we restrict ourselves to the particle-hole symmetric case.

In the weak-coupling regime in the saddle-point approximation, which includes Gaussian fluctuations of x around zero, semiclassical EDMFT Eqs. (19)–(21) read

$$\tilde{G}(\tilde{G}+\omega)^3-(\tilde{G}+\omega)^2+\alpha^2=0, \tag{23}$$

$$D_0^{-1}-D^{-1}=-T\sum_{n\geqslant 0}\frac{2g\lambda^2}{(\tilde{G}+\omega_n)^2}, \tag{24}$$

where $\tilde{G}=iG(i\omega_n)$ and $\alpha^2=\lambda^2|D|T=-\lambda^2T\int d\epsilon\rho_{ph}(\epsilon)\times[D^{-1}-D_0^{-1}-\epsilon^2]^{-1}$, so α^2 is solved for the phonon self-energy thus making the system of the saddle-point equations closed.

In the strong-coupling regime we consider two saddle-points $x=\pm x_0$. We discard fluctuations around these points (so $|D|=\beta x_0^2$), since nontrivial information is contained in the fact that we have two saddle points, and not in the Gaussian fluctuations, like it was in the case of weak coupling. EDMFT Eqs. (19) and (21) now read

$$\tilde{G}(\tilde{G}+\omega)^2-(\tilde{G}+\omega)+\tilde{G}\alpha^2=0, \tag{25}$$

$$D_0^{-1}=-T\sum_{n\geqslant 0}\frac{2g\lambda^2}{(\tilde{G}+\omega_n)^2+\lambda^2TD}. \tag{26}$$

Weak-coupling Eqs. (23) and (24) are a saddle-point expansion up to the first order in small parameter λ^2DT, and strong-coupling Eqs. (25) and (26) are up to the first order in large parameter λ^2D/T. These equations have overlapped regions of applicability, provided $T\ll 1$. This allows us to combine weak- and strong-coupling equations into a unique set of equations, controlled by the small parameter T:

$$\tilde{G}(\tilde{G}+\omega)^2-(\tilde{G}+\omega)+\tilde{G}\alpha^2=0, \tag{27}$$

$$D_0^{-1}-D^{-1}=-2g\lambda^2T\sum_{n\geqslant 0}\frac{\tilde{G}}{\tilde{G}+\omega_n}. \tag{28}$$

These are our final semiclassical EDMFT equations. They are exact in the limit $MT^2\gg\omega_0^2$, $T\ll 1$. For 3d and 2d phonons, Eqs. (27) and (28) have to be solved together with Eqs. (17) and (18), where $\xi^2=D^{-1}-D_0^{-1}$. Saddle-point Eqs. (27) and (28) are very simple; they can be solved for D and D_0 with minimal numerical effort. The left-hand side (lhs) of Eq. (27) is a third-degree polynomial, so the electron Green's function can be written as an elementary function determined by a single parameter α^2 which is a function of phonon self-energy and bare parameters of the model.

In the limits of small and large α^2 (or λ) Eqs. (27) and (28) can be solved completely for self-energies:

$$\alpha\ll 1:\quad \Sigma_{el}(i\omega_n)=\left(-\frac{\omega_n}{2}+\sqrt{1+\left(\frac{\omega_n}{2}\right)^2}\right)\alpha^2, \tag{29}$$

$$\Sigma_{ph}=-\frac{4g}{3\pi}\lambda^2. \tag{30}$$

Moreover, in the dispersionless case $\alpha^2=\lambda^2T/(\omega_0^2-[4g/3\pi]\lambda^2)$. This expression is valid everywhere except for the small region $\Delta\lambda\sim\omega_0T$ below $\lambda_c\sim\omega_0$. We consider here a disordered phase solution. In $d=3$ the disorder solution becomes unstable at $\lambda\sim\omega_0-\omega_1$ while it remains stable for all coupling in $d=2$. The self-energies in the strong-coupling regime $\alpha\gg 1$ are given by

$$\Sigma_{el}(i\omega_n)=\frac{\alpha^2}{\omega_n}, \tag{31}$$

$$\Sigma_{ph}=-\frac{g\lambda^2}{2\alpha}. \tag{32}$$

In the strong-coupling the phonon field distribution function is split into two peaks. The peak separation is $2x_0$, where $x_0=-g\lambda D_0/2$, $D=-\beta x_0^2$. In the dispersionless case $\alpha^2=([g/2]\lambda^2/\omega_0^2)^2$; this is valid when $\lambda \gg \omega_0$. This is completely similar to the previous analysis.[12]

In $d=3$ the instability to the ordered phase occurs already at small $\omega_1 \sim \omega_0^3/\beta g^2 1/\lambda^2$, so D_0 stays practically unrenormalized. In $d=2$ at $\omega_1 \sim \omega_0^3/\beta g^2 1/\lambda^2$ the system enters a regime when the phonon energy is exponentially small:

$$\Sigma_{ph}-(\omega_0-\omega_1)^2 \approx 2\omega_1 \exp\left[-\beta g \frac{\omega_1}{\omega_0^3}\lambda^2\right]. \tag{33}$$

In the limit $T\to 0$ one readily obtains the polaron formation condition, which happens at intermediate ($\lambda_c \sim \omega_0$) coupling:

$$-\frac{4g}{3\pi}\lambda_c^2 D_0=1, \tag{34}$$

where $D_0=\omega_0^{-2}$ in the dispersionless case, but has to be found numerically for interacting phonons.

III. 3D PHONONS

In this section we compare our semiclassical solution to the exact QMC results.[7] The saddle-point equations we derived are exact when $(2\pi T)^2 M\omega_0^{-2} \gg 1$ and $Tt^{-1} \ll 1$. The QMC results,[7] however, were obtained for $(2\pi T)^2 M\omega_0^{-2} \approx 2.5$ and $Tt^{-1} \approx 0.13$. We want to show that even in these cases when the parameters controlling the saddle-point equations are relatively close to 1, the semiclassical solution, even without including the refinements outlined in Ref. 10, not only captures all the qualitative trends of the exact solution, but in many instances is quantitatively close to it.

We study the case of three-dimensional phonons. We use the same parameters as in Ref. 7: inverse temperature $\beta=8$, the phonon band is centered at $\omega_0=0.5$, electrons have double spin degeneracy $g=2$ and hopping amplitude $t=1$, and the phonon mass $M=1$. The electron band is half filled. To model 3D phonons, a semicircular DOS, Eq. (12), is used. We present the solution of Eqs. (27) and (28), and Eq. (17).

In every figure in this section we plot both our own and QMC curves. Our results are plotted using solid or dashed lines only, without symbols. QMC graphs are presented using dotted lines and always with symbols.

A local instability, starting from the disordered phase, takes place within EDMFT when as discussed in Ref. 7 the effective phonon frequency $\omega^*=\sqrt{(\omega_0-\omega_1)^2+\Pi}$, given by the pole in the phonon Green's function, becomes equal to zero. The phonon mode softening for different values of the phonon dispersion are shown in Fig. 1. ω^* is plotted versus

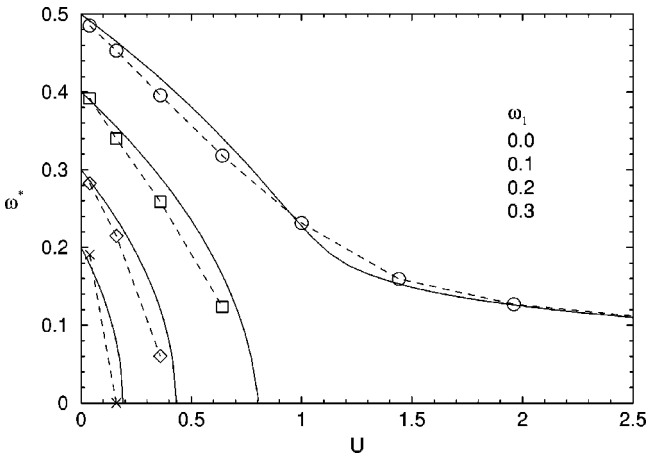

FIG. 1. $d=3$. Effective phonon frequency ω^* as a function of λ^2/ω_0^2 at $\omega_1=0.0$, 0.1, 0.2, and 0.3. Comparison to QMC results.

the quantity characterizing the effective interaction: $U=\lambda^2/\omega_0^2$. The effective electron-electron interaction, mediated by phonons, is given by $U_{eff}=\lambda^2 D_0$, evaluated at zero frequency. When the phonon dispersion vanishes, $U_{eff}=U$. The upper curve in Fig. 1 corresponds to the dispersionless case. On the other hand, we find this is not the best way to detect an instability to an ordered phase and we discuss in Appendix D an alternative way to compute within EDMFT the phonon self-energy which retains momentum dependence.

The equations in Sec. II do not include the possibility of the phonon field symmetry breaking. They need to be modified to describe long-range ordering,[9] and we implement this in Sec. V. A well-known property of mean-field theories is that they allow the analytic continuation of mean-field solutions beyond the parameter regime where they are stable. This was very fruitful in the understanding of the paramagnetic Mott insulating phase which is unstable to ferromagnetism.[1] As was done by the QMC method in Ref. 7, we study the continuation of the EDMFT equations beyond the paramagnetic phase. It may, hopefully, be understood as a metastable phase. This requires some care since the instability to a charge ordered phase is signaled by a singularity appearing in the integrand in Eq. (15) and this instability causes D to acquire an imaginary part. As in Ref. 7, we take the principal part of the integrand, the imaginary part of D_0, being equal to zero in every numerical iteration loop, which allows us to compare our results with the results of the QMC method.

A. Weak coupling

The finite dispersion treated within DMFT renormalizes D_0 [see Fig. 2(a)]. Since the effective electron-electron interaction is proportional to D_0, the electron self-energy is enhanced as well [see Fig. 2(b)]. While the features of the exact solution are qualitatively well reproduced in the semiclassical approach, the approach lacks quantitative agreement. Weak coupling is the worst case. The quantitative agreement is better for intermediate and strong-coupling.

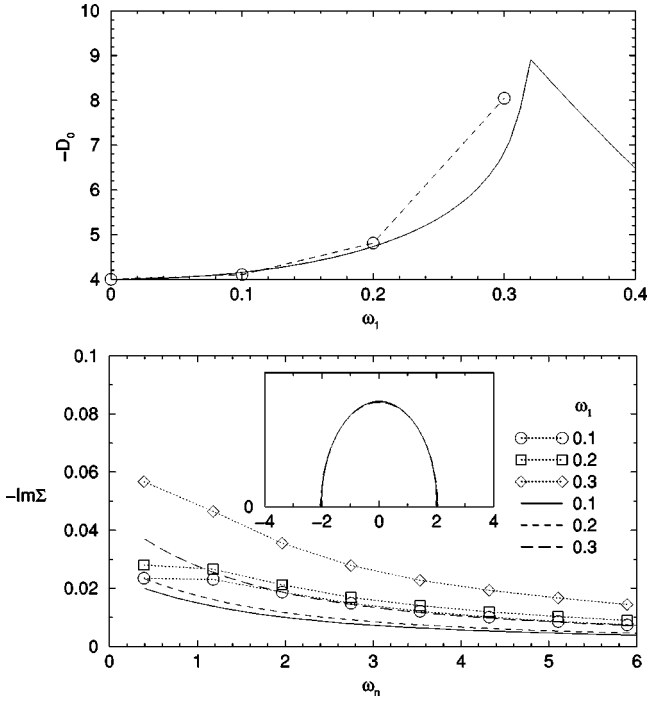

FIG. 2. $d=3$, weak coupling $\lambda=0.2$, comparison to QMC results. (a) The bare phonon Green's function. (b) The imaginary part of the electron self-energy with the spectral function in the inset. $\omega_1=0.1$, 0.2, and 0.3.

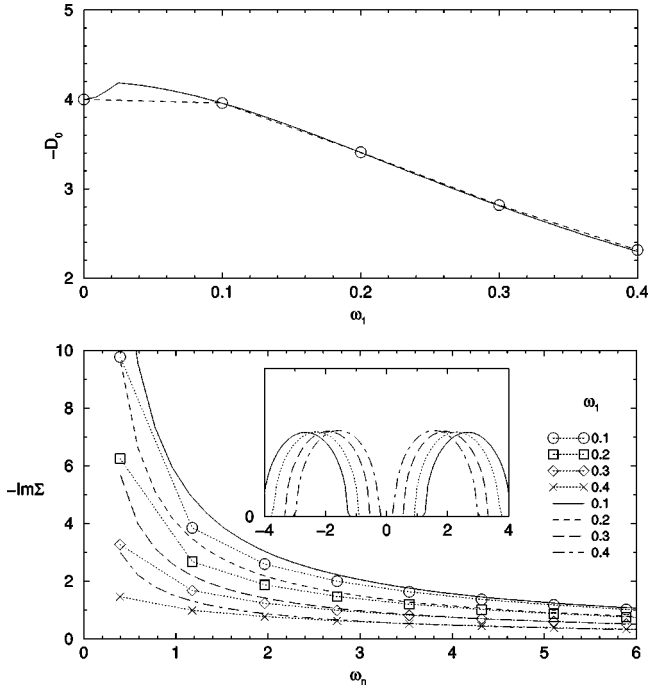

FIG. 3. $d=3$, strong coupling, $\lambda=0.8$. (a) Bare phonon Green's function. (b) Imaginary part of the electron self-energy with the spectral function in the inset. $\omega_1=0.1$, 0.2, 0.3, and 0.4.

B. Strong coupling

In the strong-coupling regime as dispersion increases, D_0 renormalizes downward [see Fig. 3(a)], together with the electron self-energy [see Fig. 3(b)]. For strong coupling the quantitative agreement with the QMC results is very good.

C. Intermediate coupling

At intermediate coupling, the system is in a crossover between weak- and strong-coupling regimes. As ω_1 increases, the effective electron-electron interaction first becomes stronger, and D_0 and the electron self-energy increases, like at weak coupling. At $\omega^*=0$, the behavior changes to the reverse, and the picture is similar to the strong-coupling case. This is illustrated in Fig. 4(a) and Fig. 4(b).

IV. 2D PHONONS

In the previous section we calculated various functions at different parameters in the 3*d* case. The saddle-point approximation is exact in the limit of infinite mass M and zero temperature T. At finite M and T the applicability of the method in a wide region of parameters was established in the previous section by comparison to QMC data. In this section we study the 2d phonon case [Eqs. (27) and (28) and Eq. (18)] in the same range of parameters.

Unlike the 3d case, the 2d disorder solution is locally stable, and we focus on this solution in this section. As we will show in Sec. V the EDMFT in dimensions $d<4$ gives rise to a first-order transition at a critical coupling strength. We study the disordered state solution continued along the second-order transition branch, which is skipped in the first-order transition.

In the EDMFT approach, $d=2$ appears as a lower critical dimension for a finite temperature second-order transition. This result describes accurately the situation with order parameters possessing a continuous symmetry, but it is a spurious consequence of the inability of a local approximation to generate spatial anomalous dimensions in the cases where order breaks a discrete symmetry.

First we illustrate the exponential softening of the collective mode: in Fig. 5 we plot effective frequency ω^* versus U. Figure 5 should be compared to Fig. 1 (3*d* case). In the latter the curves hit the U axis, which implies a second-order transition. In Fig. 5 the curves rather gradually approach the U axis, never crossing it.

Phonons generate an effective electron-electron interaction $\sim\lambda^2 D_0$, so we are especially interested in D_0 behavior. We investigate the 2d system for similar sets of parameters as we did in the 3d case. We obtained the plots for weak, intermediate-, and strong-coupling regimes in Figs. 6–8.

The behavior of the 2d system is very similar to that of the 3d system before the energy of the phonon mode vanishes. In all cases D_0 gets renormalized, as the dispersion and consequently the effective interaction increases. The electron self-energy enhances correspondingly. The only difference is the rate of D_0 renormalization in the weak, strong, and intermediate couplings. D_0 renormalizes faster at larger λ (see Fig. 9), since electrons are stronger coupled to phonons.

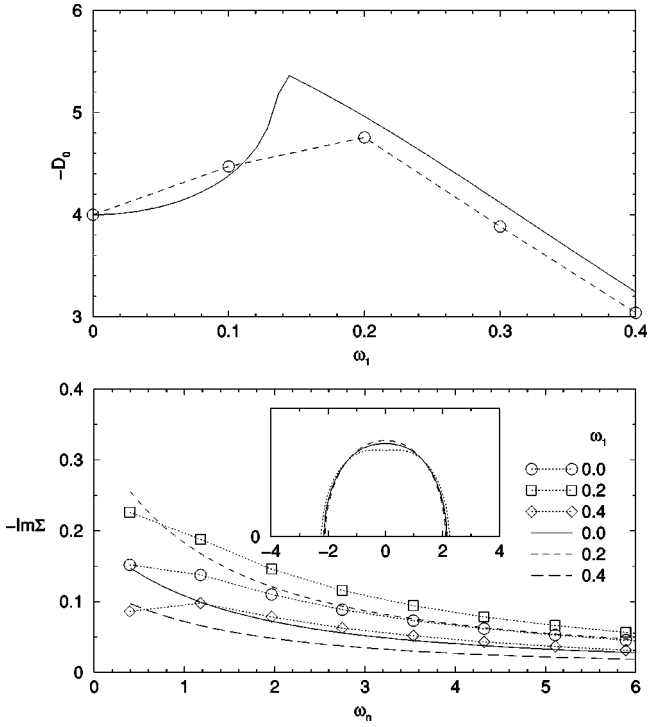

FIG. 4. $d=3$, intermediate coupling $\lambda=0.4$, comparison to QMC results. (a) Bare phonon Green's function. (b) Imaginary part of the electron self-energy with the spectral function in the inset. $\omega_1=0.0$, 0.2, and 0.4.

V. ORDERED PHASE AND CRITICAL TEMPERATURE

We now turn to the generalization of the EDMFT equations to the ordered phase.[9] For simplicity we will consider a classical model. This is justified, since in the semiclassical limit we can always integrate out the electrons, reducing EDMFT equations to classical mean-field equations. For instance, tracing out the electrons and performing a static approximation in the electron-phonon field leaves us with an action of the form (neglecting terms of order ϕ^6 and higher):

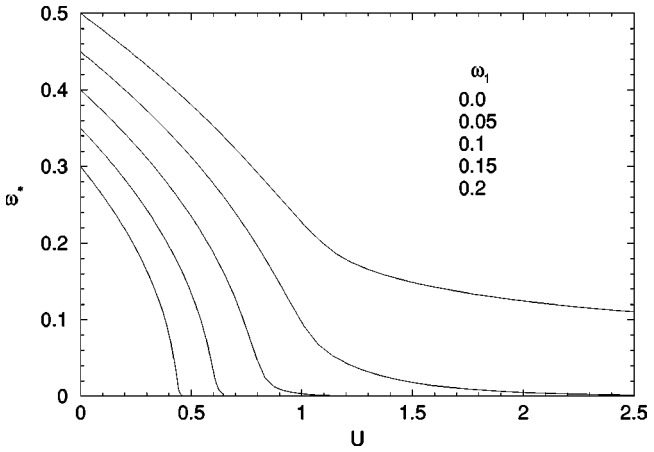

FIG. 5. $d=2$. Effective phonon frequency ω^* as a function of λ^2/ω_0^2 at $\omega_1=0.0$, 0.05, 0.1, 0.15, and 0.2.

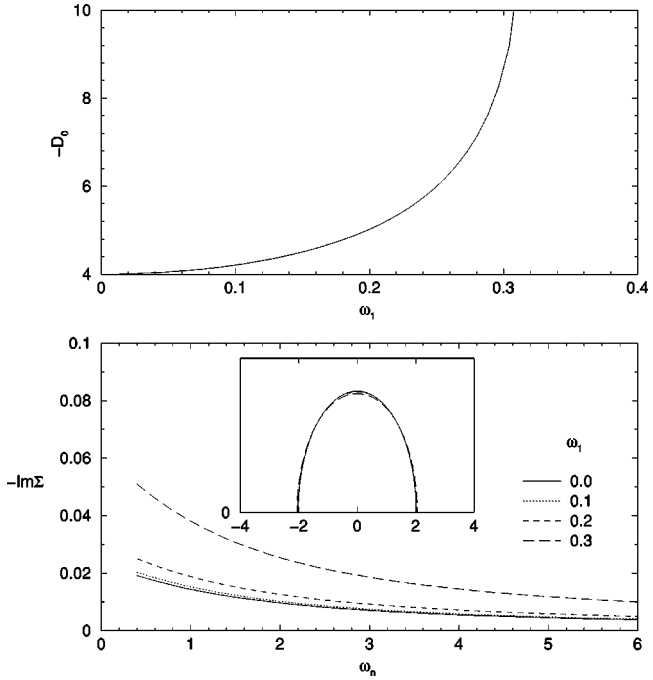

FIG. 6. $d=2$, weak coupling, $\lambda=0.2$. (a) The bare phonon Green's function. (b) The imaginary part of the electron self-energy with the spectral function in the inset. $\omega_1=0.0$, 0.1, 0.2, and 0.3.

$$S[\phi]=\sum_i \frac{r}{2}\phi_i^2+\frac{U}{4}\phi_i^4-\sum_{ij}\ \phi_i\frac{J_{ij}}{2}\phi_j$$

$$=S_{loc}[\phi]-\sum_{ij}\ \phi_i\frac{J_{ij}}{2}\phi_j\,. \tag{35}$$

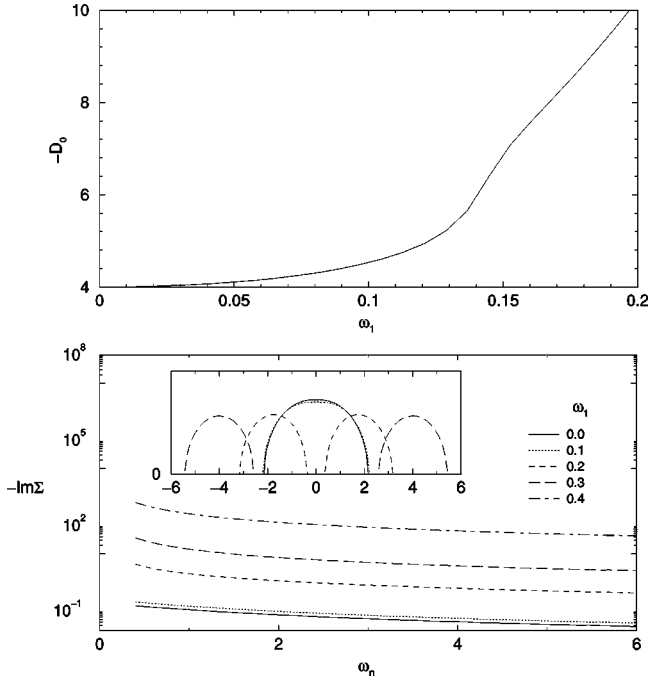

FIG. 7. $d=2$, intermediate coupling, $\lambda=0.4$. (a) The bare phonon Green's function. (b) The imaginary part of the electron self energy with the spectral function in the inset. $\omega_1=0.0$, 0.1, 0.2, 0.3, and 0.4.

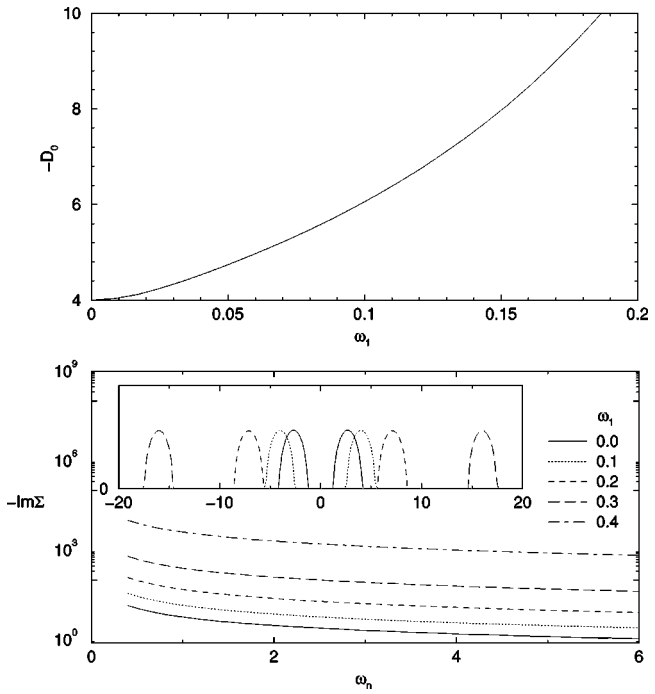

FIG. 8. $d=2$, strong coupling, $\lambda=0.8$. (a) The bare phonon Green's function. (b) The imaginary part of the electron self-energy with the spectral function in the inset. $\omega_1=0.0$, 0.1, 0.2, 0.3, and 0.4.

To extend the EDMFT approach to the ordered phase it is useful to write the Baym-Kadanoff functional for the action,

$$\Gamma[m,D]=-\frac{1}{2}\mathrm{Tr}\ln D+\frac{1}{2}\mathrm{Tr}D_0^{-1}D+\frac{1}{2}mD_0^{-1}m+\Phi[m,D], \tag{36}$$

where Φ is a sum of all two-particle irreducible diagrams constructed from phonon Green's functions D, phonon field expectation value m, and the four-legged interaction vertex $-3!U$. We could also say that Φ is a sum of all two-particle irreducible diagrams constructed from phonon Green's functions D and four-, three-, two-legged vertices plus the first

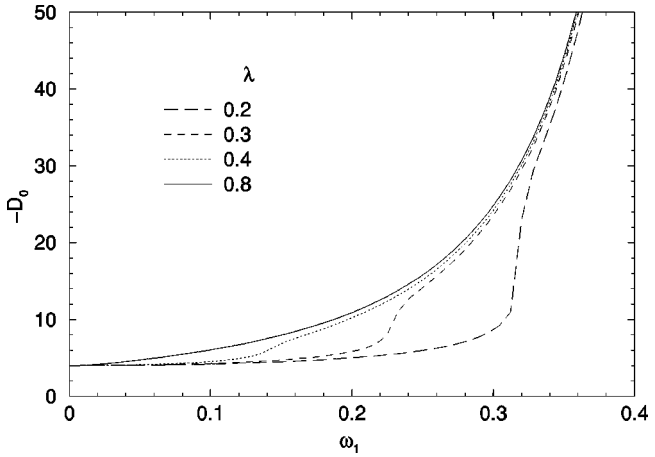

FIG. 9. $d=2$, bare phonon Green's function, $\lambda=0.2$, 0.3, 0.4, and 0.8.

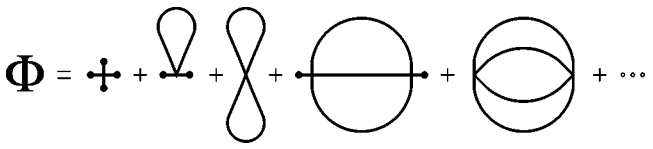

FIG. 10. Diagrammatic expansion of Φ up to the first two orders in U.

diagram shown in Fig. 10, which contains no propagators. The vertices yield factors of $-3!U$, $-3!Um$, $-3Um^2$, and $-\frac{1}{4}Um^4$ for four-, three-, two- and zero-legged vertices, respectively. Each diagram in Φ has an extra -1 factor.

In Fig. 10 we drew first- and second-order (in U) diagrams entering Φ. The extended DMFT equations in the ordered phase are derived by making the local approximation on Φ in the Baym-Kadanoff functional and solving the stationary conditions for the magnetization and the local propagator resulting from the stationarity of Eq. (36) after this local approximation is made. In the local approximation the leading terms in a perturbative expansion in the quartic coupling are given by $\Phi=\frac{1}{4}Um^4+\frac{3}{2}UDm^2+\frac{3}{4}UD^2-3U^2D^3m^2-\frac{3}{4}U^2D^4+\ldots$.

Stationarity of the functional in Eq. (36) would give exact equations for D and m. In the local approximation these equations reduce to EDMFT equations in zero magnetization and therefore generalize those to the ordered phase.[9] They are given by

$$m(r-J_{q=0})+\frac{\delta\Phi}{\delta m}=0,$$

$$D=\sum_q\left[r-J_q+2\frac{\delta\Phi}{\delta D}\right]^{-1}, \tag{37}$$

where only local graphs are included in Φ. Diagram series equivalent to the first equation are shown in Fig. 11.

For the practical solution of the EDMFT, Eq. (37), it is useful to follow the dynamical mean-field procedure of introducing an impurity local effective action[1,17] to sum up the graphs generated by the functional for Φ and its functional derivatives $\delta\Phi/\delta D$ and $\delta\Phi/\delta m$ in terms of the cavity fields h and Δ. The effective action

$$S_{EDMFT}[\phi]=S_{loc}[\phi]-h\phi-\frac{\Delta}{2}\phi^2 \tag{38}$$

generates the correct local quantities provided that the Weiss fields h and Δ are chosen to obey the EDMFT self-consistency conditions:

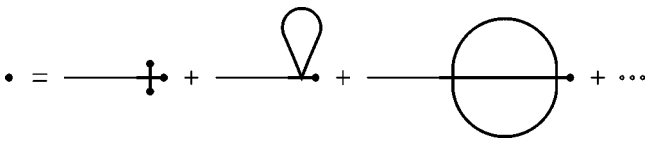

FIG. 11. Diagrammatic expansion of m up to the first two orders in U. Thin lines are the free phonon propagator D_0, thick lines are the full phonon propagator, and a full dot stands for m.

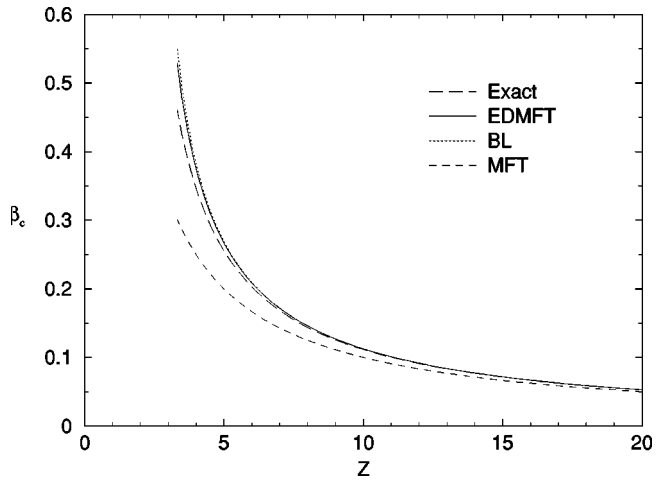

FIG. 12. Top to bottom: BL, EDMFT, exact solution, and MFT; critical J_c vs nearest-neighbors number z.

$$r-\Delta-D^{-1}=-2\frac{\delta\Phi}{\delta D}, \tag{39}$$

$$h=-m(r-\Delta)-\frac{\delta\Phi}{\delta m}. \tag{40}$$

Equations (37) and Eqs. (39) and (40) are a closed set of EDMFT equations, describing both ordered and disordered phases of the classical system, Eq. (35):

$$D=\sum_q\,[D^{-1}+\Delta-J_q]^{-1}, \tag{41}$$

$$S_{EDMFT}[\phi]=S_{loc}[\phi]-m(J_{q=0}-\Delta)\phi-\frac{\Delta}{2}\phi^2, \tag{42}$$

$$m=\langle\phi\rangle_{S_{EDMFT}}, \tag{43}$$

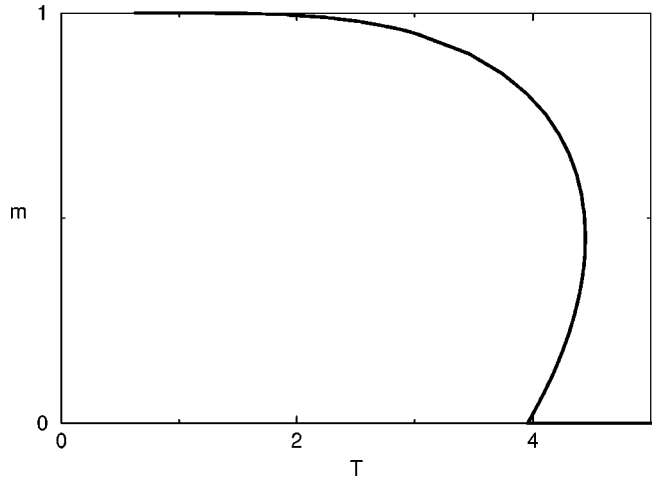

FIG. 13. Magnetization vs temperature on a cubic lattice. There are three branches at $3.96<T<4.45$: $m_3>m_2>m_1=0$; m_1 and m_3 are physical solutions, while m_2 is not. Classical ±1 spin Ising model.

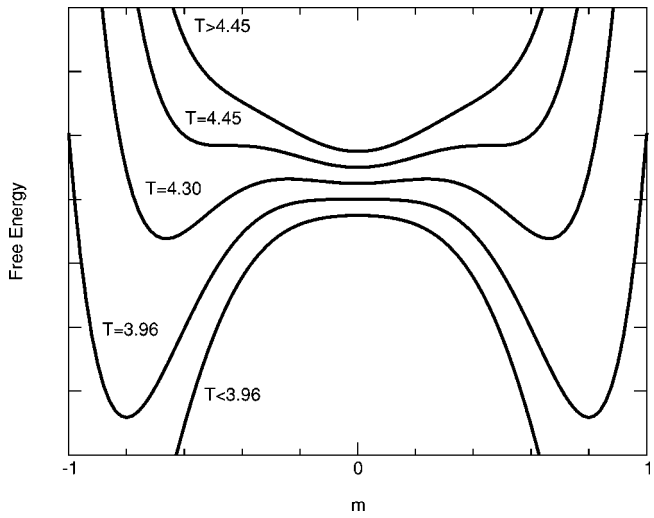

FIG. 14. Free-energy evolution with T. The free energy has a single minimum ($m=0$) above $T=4.45$; at $T=4.45$ the solution bifurcates at $m=0.45$. There are free extrema at $3.96<T<4.45$ corresponding to $0=m1<m2<m3$. As T approaches $T_c=3.96$, $m2$ merges with $m1$.

$$D=\langle\phi^2\rangle_{S_{EDMFT}}-m^2. \tag{44}$$

The equations above are consistent in describing the transition: magnetization vanishes in the ordered phase, and divergence of spin susceptibility across the transition occurs at the same critical temperature.

When $U\to\infty$, $r\to-\infty$, and $U/r=-1$ the system, described by the action of Eq. (35), reduces to a classical Ising model with spin values ±1. In this limit the standard Weiss mean-field equation

$$m=\tanh mJ_{q=0} \tag{45}$$

can be compared with the EDMFT equations which now read

$$m=\tanh m(J_{q=0}-\Delta),$$

$$1-m^2=\sum_q\,[(1-m^2)^{-1}+\Delta-J_q]^{-1}. \tag{46}$$

We will also compare the EDMFT equations to an extension of mean-field theory (MFT) from Bloch and Langer (BL):[13]

$$M_1=\int_{-\infty}^{+\infty}dx(2\pi G_2)^{-1/2}\exp\left[-\frac{(M_1J_{q=0}-x)^2}{2G_2}\right]\tanh x, \tag{47}$$

$$M_2=\int_{-\infty}^{+\infty}dx(2\pi G_2)^{-1/2}\exp\left[-\frac{(M_1J_{q=0}-x)^2}{2G_2}\right](\cosh x)^{-2}, \tag{48}$$

$$G_2=\sum_q\,\frac{J_q}{1-J_qM_2}, \tag{49}$$

where M_1 is the magnetization. It can be shown that EDMFT counts (without overcounting) more terms in diagrammatic expansion of various physical quantities, like correlation function or free energy, than the BL method. One can also check that for the classical ± 1 spin model, EDMFT gives a better estimate for T_c than the BL method.

We computed the critical temperature T_c for the Ising model on a Bethe lattice with finite coordination following the paramagnetic solution until it disappears using the different approximations described in this section. The results are shown in Fig. 12. The EDMFT result shows significant improvement over MFT, and is slightly better than the BL method. Some more technical details comparing the approximation schemes are relegated to Appendix A.

In spite of the quantitative improvement of T_c, the order of the transition is incorrectly given by the EDMFT approximation. In Fig. 13 we present the result of solving EDMFT equations for the simplest ± 1 spin model in $d=3$. We plotted magnetization as a function of temperature. At sufficiently low temperature the solution consists of three branches with magnetizations $m_3 > m_2 > m_1 = 0$. These branches are extrema of the free energy, which is shown schematically in Fig. 14. m_3 and m_1 correspond to local minima in the free energy, while m_2 corresponds to a local maximum and is unphysical. The transition is clearly of the first order. The order of the transition does not change up to $d=4$.

The inability of EDMFT to predict the correct order of the transition is related to the inability of a local theory to produce anomalous dimensions, and persists in quantum problems when the dynamical critical exponent and the dimensionality are such that they require the introduction of spatial anomalous dimensions. Details are given in Appendices B and C.

VI. CONCLUSION

We have performed a semiclassical analysis of the EDMFT equations for a simple fermion boson model. Comparison with earlier QMC treatments of the same problem reveals that this method reproduces semiquantitatively all the trends found in the previous study.[7] It can be used, therefore, in the study of more complicated systems, such as fermions interacting with spin fluctuations. We have also investigated this approach in the ordered phase revealing some inadequacies of the approach which are closely related to the existence of anomalous dimensions in finite-dimensional systems. Since this nontrivial k dependence, which is characteristic of low-dimensional systems, cannot be generated by a local theory, EDMFT produces spurious results such as the existence of a first-order phase transition in $d<4$. Since at zero temperature the dynamical critical exponent is such that in two dimensions an ansatz without anomalous dimensions is internally consistent,[5] a continuation of the disordered state, beyond the first-order phase transition, might be useful to study this system. In this spirit we pointed out that a continuation of the EDMFT, at finite temperature, suitably interpreted, gives improved estimates of the critical temperature compared to the simplest mean-field treatment or the Bloch-Langer method.[13] It could be used to obtain better estimates of ferromagnetic transition temperatures where spatial fluctuations of the order parameter substantially decrease the Curie temperature below the DMFT estimates. This is the case of bcc iron,[18] a problem which will require a more realistic investigation of EDMFT. Further investigation of the quantum problem will require zero-temperature methods which go beyond the semiclassical approximation.

ACKNOWLEDGMENT

This research was supported by the Division of Materials Science of the National Science Foundation under Grant No. DMR 89-15895-01.

APPENDIX A: CRITICAL TEMPERATURE

The transition to the ordered state for a classical model in the BL method is signaled by the divergence in the zero-momentum term in the sum:

$$G_2 = \sum_q \frac{J_q}{1 - J_q M_2}. \tag{A1}$$

This equation is analogous to the self-consistency equation of the EDMFT, as it arises when summing ring diagrams. M_2 is a vertex and J_{ij} is a line in the ring diagram. $G_2(i)M_2$ is the sum of all ring diagrams which covers the site i. M_2 and G_2 are related to D in EDMFT:

$$D = M_2 + M_2 G_2 M_2. \tag{A2}$$

Below we explicitly sum ring graphs on a Bethe lattice to express G_2 through M_2. We introduce notations $\tilde{G}_2(i)$ and $Q(i)$: $\tilde{G}_2(i)$ equals $G_2(i)$ when the latter is computed on a lattice with all but one bond cut out from site i. $Q(i)M_2$ includes those diagrams from $\tilde{G}_2(i)M_2$ which have only one vertex belonging to site i.

The following relations can be established:

$$\begin{aligned} G_2 = {} & z\tilde{G}_2 + z\tilde{G}_2(z-1)M_2\tilde{G}_2 \\ & + z\tilde{G}_2(z-1)M_2\tilde{G}_2(z-1)M_2\tilde{G}_2 + \ldots, \end{aligned} \tag{A3}$$

$$\tilde{G}_2 = Q + QM_2Q + QM_2QM_2Q + \ldots, \tag{A4}$$

$$\begin{aligned} Q = {} & JM_2J + JM_2(z-1)\tilde{G}_2M_2J \\ & + JM_2(z-1)\tilde{G}_2M_2(z-2)\tilde{G}_2M_2J \\ & + JM_2(z-1)\tilde{G}_2M_2(z-2) \\ & \times \tilde{G}_2M_2(z-2)\tilde{G}_2M_2J + \ldots, \end{aligned} \tag{A5}$$

where z is the number of nearest neighbors, and J is a bond on the lattice.

Summing geometrical series, we obtain

$$G_2 = \frac{z\tilde{G}_2}{1-(z-2)M_2\tilde{G}_2}, \tag{A6}$$

$$\tilde{G}_2=\frac{Q}{1-M_2Q}, \tag{A7}$$

$$Q=J^2M_2\frac{1+M_2\tilde{G}_2}{1-(z-2)M_2\tilde{G}_2}. \tag{A8}$$

Solving these equations we get

$$G_2=\frac{zQ}{1-zM-2Q}, \tag{A9}$$

$$Q=\frac{1-\sqrt{1-(z-1)(2M_2J)^2}}{(z-1)2M_2}. \tag{A10}$$

Equation (A9) and Eq. (A10) solve G_2 for M_2.

Curves J_c vs z for the BL theory and EDMFT, together with the MFT solution $J_c=1/z$, are presented in Fig. 12 and compared to the exact solution:

$$J_c=\frac{1}{2}\ln\frac{z}{z-2}. \tag{A11}$$

APPENDIX B: ORDER OF THE PHASE TRANSITION

Here we prove that the EDMFT equations give a transition of the first order for $d<4$ and of the second order in the higher dimensions. For classical phonons EDMFT equations read

$$m(r-J_{q=0})=-\frac{\delta\Phi[m,D]}{\delta m},$$

$$D=\sum_q\left[r+2\frac{\delta\Phi[m,D]}{\delta D}-J_q\right]^{-1}. \tag{B1}$$

It is easily seen that

$$\left.\frac{\delta^2\Phi[m,D]}{\delta m^2}\right|_{m=0}=2\frac{\delta\Phi[0,D]}{\delta D}. \tag{B2}$$

Solving Eq. (B1) for r using the above relation for derivatives, up to the second order in m, we have

$$-\frac{m^2}{2}D''|_{m=0}=D|_{m=0}-\sum_q\left[\left(2\frac{\delta^2}{\delta D^2}-\frac{1}{6}\frac{\delta^4}{\delta m^4}\right)\times\Phi[m,D]|_{m=0}m^2+J_{q=0}-J_q\right]^{-1}. \tag{B3}$$

The coefficient in front of m^2 in the right-hand side (rhs) is positive. The lhs of Eq. (B3) is $\propto m^2$, while the rhs has two contributions, one $\propto m^{d-2}$ and the other $\propto\delta\beta$, where $\delta\beta=\beta-\beta_c$. For $d<4$ the term $\propto m^{d-2}$ is dominant and $\delta\beta\propto -m^{d-2}<0$. A negative $\delta\beta$ implies the first-order transition. For $d>4$ the term m^2 from the lhs becomes dominant and $\delta\beta\propto m^2>0$. This is the usual mean-field behavior resulting in a second-order transition.

We showed that in a classical model the transition is of the first order below the upper critical dimension. The same is true for a quantum transition as well. We show it in Appendix C considering the large N limit.

As discussed earlier in connection with the order of the transition, this artifact of the EDMFT results from the inability of a local theory to capture physics that requires the introduction of anomalous dimensions. In spite of this shortcoming, when properly interpreted, EDMFT results in improved estimates of the critical temperature relative to DMFT.

APPENDIX C: QUANTUM PHASE TRANSITION

In this Appendix we investigate the phase transition in the quantum version of the ϕ^4 model. We compare EDMFT and a full lattice model using the large N technique. We will show that above the upper critical dimension $d>d_{uc}=4-z$ the exact critical exponents and the critical exponents obtained in EDMFT coincide. Below d_{uc} the EDMFT and the lattice model exhibit different critical exponents. In the EDMFT the transition is of the first order for $\frac{1}{2}d_{uc}<d<2$ and of the second order otherwise. The transition is of the second order in the lattice case. Moreover, in EDMFT the exponents have a universal value for $d<\frac{1}{2}d_{uc}$ and a nonuniversal value for $\frac{1}{2}d_{uc}<d<d_{uc}$.

The lattice model is described by the action

$$S=\frac{1}{2}D_0^{-1}\phi^2+\frac{U}{4}(\phi^2)^2, \tag{C1}$$

where $D^{-1}_{0\omega,q}=r+|\omega|^{2/z}+q^2$, $\phi^2=\Sigma_{a=1}^N\phi_a^2$, $U=u/N$, and r is a variable parameter which drives the phase transition. Corresponding EDMFT equations are

$$mD^{-1}_{0\omega,q=0}+\frac{\delta\Phi[m,D]}{\delta m}=0, \tag{C2}$$

$$D=\sum_q\left[D_{0q}^{-1}+2\frac{\delta\Phi[m,D]}{\delta D}\right]^{-1}. \tag{C3}$$

The functional $\Phi[m,D]$ includes all two-particle irreducible diagrams which are constructed from (see Fig. 10) the magnetization m (dot), the particle propagator D (line), and the interaction term U (four-legged vertex). Φ satisfies the following equation:

$$\left.\frac{\delta^2\Phi[m,D]}{\delta m^2}\right|_{m=0}=2\frac{\delta\Phi[0,D]}{\delta D}. \tag{C4}$$

Expanding Φ in small m and using Eq. (C4) we write EDMFT equations as

$$D^{-1}_{0\omega,q=0}+2\frac{\delta\Phi[0,D]}{\delta D}+\frac{1}{6}\frac{\delta^4\Phi[m,D]}{\delta m^4}|_{m\to0}m^2=0, \tag{C5}$$

FIG. 15. $1/N$ expansion of Γ. All diagrams are of the order $1/N$.

$$D_\omega = \int_0^\Lambda dq^d \left[|\omega|^{2/z} + q^2 + \left\{ 2\Gamma - \frac{1}{6}\frac{\delta^4\Phi[m,D]}{\delta m^4}\bigg|_{m\to 0} \right\} m^2 \right]^{-1}, \quad \text{(C6)}$$

where $\Gamma = \delta^2\Phi[0,D]/\delta D^2$.

Let D_{0c}, D_c, and r_c be values of D_0, D, and r respectively, in the transition point. Subtracting $D^{-1}_{0c\omega,q=0} + 2(\delta\Phi[0,D_c]/\delta D) = 0$ from Eq. (C5) and keeping lowest-order terms, we have

$$\delta r + 2\Gamma\,\delta D + \frac{1}{6}\frac{\delta^4\Phi}{\delta m^4} m^2 = 0, \quad \text{(C7)}$$

where $\delta r = r - r_c$, and $\delta D = D - D_c$. This equation provides a relation between the variation of the driving term r and the order parameter m. We will show that for $d > d_{uc}$ the last term in the left-hand side wins over the second term, the transition is mean-field-like. The second term becomes important and determines the character of the transition for $d < d_{uc}$.

We will consider the large N limit up to the order of $1/N$. Diagrams which enter Γ are chains of bubbles (see Fig. 15), which can be summed as a geometrical series:

$$\Gamma = \frac{1}{N}\left(\frac{u}{2} + \frac{u}{1 + \frac{u}{2}\chi} \right), \quad \text{(C8)}$$

where $\chi_\omega \sim \int d\nu D_\nu D_{\nu+\omega}$ in the quantum problem or $\chi = D^2$ in the classical problem. The only term of the order $1/N$ which enters $\delta^4\Phi/\delta^4 m$ is $6u/N$. All other terms are of order $O(1/N^3)$.

Equation (C7) and Eq. (C8) holds in case of a lattice as well, but D now depends on both momentum and frequency, and summations now run over wave vectors as well. The upper and lower critical dimensions are determined by the convergence of integrals $\mathrm{Tr}\,\delta D$ and $\mathrm{Tr}\,D$ in the ultraviolet and infrared limits, respectively:

$$\mathrm{Tr}\,\delta D \sim \int d\omega dq \frac{q^{d-1}}{(|\omega|^{2/z} + q^2)^2}, \quad \text{(C9)}$$

$$\mathrm{Tr}\,D \sim \int d\omega dq \frac{q^{d-1}}{(|\omega|^{2/z} + q^2)}. \quad \text{(C10)}$$

These equations are the same for the mean-field and lattice models, they yield the upper critical dimension $d_{uc} = 4 - z$ and the lower critical dimension $d_{lc} = 2 - z = d_{uc} - 2$.

We first consider EDMFT. In a crude way one can estimate:

$$d > 2, \quad D_\omega \sim \int d^d q (|\omega|^{2/z} + q^2)^{-1} \sim (d-2)^{-1}(\Lambda_q^{(d-2)} - |\omega|^{(d-2)/z}), \quad \text{(C11)}$$

$$d < 2, \quad D_\omega \sim -(d-2)^{-1}|\omega|^{(d-2)/z} \quad \text{(C12)}$$

and

$$d > 2, \quad \chi_\omega \sim \int d\nu D_\nu D_{\nu+\omega} \sim (d-2)^{-2}|\omega|^{(d-2)/z+1}, \quad \text{(C13)}$$

$$d < 2, \quad \chi_\omega \sim -(d-2)^{-2}\left(2\frac{d-2}{z} + 1 \right)^{-1} |\omega|^{2(d-2)/z+1}. \quad \text{(C14)}$$

Λ_q is a momentum cutoff. We see from Eq. (C14) that for $d < d_{uc}/2$ the susceptibility χ_ω is divergent at low frequency, it leads to a universal critical behavior for $d < d_{uc}/2$, as follows from the self-energy calculation below. The self-energy in the large N limit is $\delta\Sigma \sim 2\Gamma D$:

$$\frac{d_{uc}}{2} < d < d_{uc}, \quad \Sigma_\omega \sim \frac{1}{N}(d-2)^{-1} u |\omega|^{(d-2)/z+1} \quad \text{(C15)}$$

$$d_{lc} < d < \frac{d_{uc}}{2}, \quad \Sigma_\omega \sim \frac{1}{N}\int d\nu \chi_\nu^{-1} D_{\nu+\omega} \sim \frac{1}{N}(d-2)\left(2\frac{d-2}{z} + 1 \right)|\omega|^{-(d-2)/z}. \quad \text{(C16)}$$

In a similar way we can calculate a contribution from m to $\Gamma\,\delta D$,

$$\frac{d_{uc}}{2} < d < d_{uc}, \quad \Gamma\,\delta D \sim \frac{1}{N}(d-2)^{-1} u m^{d-2+z}, \quad \text{(C17)}$$

$$d_{lc} < d < \frac{d_{uc}}{2}, \quad \Gamma\,\delta D \sim \frac{1}{N}(d-2)\left(2\frac{d-2}{z} + 1 \right) m^{-d+2}. \quad \text{(C18)}$$

This result together with Eq. (C7) suggests that the transition is the first order for $\frac{1}{2}d_{uc} < d < 2$.

Now we consider the lattice model:

$$\chi_{\omega,q} \sim \int d\nu d^d p [|\nu+\omega|^{2/z} + (p+q)^2]^{-1} (|\nu|^{2/z} + p^2)^{-1} \sim (d+z-4)^{-1}(|\omega|^{2/z} + q^2)^{(d+z)/2-2}, \quad \text{(C19)}$$

$$\Sigma_{\omega,q} \sim \frac{1}{N}\int d\nu dp \chi^{-1}_{\nu,p} D_{\nu+\omega,p+q} \sim \frac{1}{N}(d+z-4)(|\omega|^{2/z}\ln|\omega| + q^2 \ln q). \quad \text{(C20)}$$

In this case the frequency-dependent part of the self-energy can be conveniently exponentiated to yield $D \sim [|\omega|^{2/z}$

$+q^{2-\eta}]^{-1}$ with $\tilde{z}=2-N^{-1}(d-d_{uc})c_1(d)$ and $\eta=-N^{-1}(d-d_{uc})c_2(d)$, where $c_1(d)$ and $c_2(d)$ are some smooth functions of d.

We also calculate a contribution from m to $\Gamma\delta D \sim N^{-1}(d-d_{uc})m^2\ln m$. It yields $\delta r\sim m^{1/\beta}$ with $\beta=\frac{1}{2}+(d-d_{uc})(1/N)c_3(d)$. The transition is the second order in this case.

APPENDIX D: INSTABILITY ANALYSIS

Let us consider a very general electron-phonon Hamiltonian which describes an electron-phonon system with electron-electron interaction (local or long range), electron-phonon interaction, and phonon-phonon interaction (phonon unharmonicity). We can always use a Hubbard-Stratonovich decoupling on electron-electron interaction, so we assume that information about long-range electron-electron interaction is stored in the phonon dispersion and we will not write the long-range interaction explicitly. We can introduce a source-dependent action S where the sources are coupled to different fields. The free energy $W=-\ln\int e^S$ is the generating functional for expectation values of those fields:

$$\begin{aligned}S=&\int dxdx' c^\dagger_\sigma(x)G^{-1}_{0\sigma}(x-x')c_\sigma(x')\\&+\tfrac{1}{2}\phi(x)D_0^{-1}(x-x')\phi(x')\\&+\delta(x-x')(Un_\uparrow(x)n_\downarrow(x)+V_4\phi^4(x)\\&+\lambda\phi(x)c^\dagger_\sigma(x)c_\sigma(x))-J_\sigma(x,x')c^\dagger_\sigma(x)c_\sigma(x')\\&-\tfrac{1}{2}\phi(x)K(x,x')\phi(x')-\delta(x-x')L(x)\phi(x).\end{aligned}\tag{D1}$$

The x variable includes both space and time in the above formula and repeated indices imply summation. Expectation values of the fields coupled to the sources are given by

$$G=\frac{\delta W}{\delta J},\quad K=2\frac{\delta W}{\delta K},\quad m=\frac{\delta W}{\delta L},\tag{D2}$$

Exact Green's functions correspond to the limit of zero sources. To study phase transitions, like the transition when the phonon field acquires a nonzero expectation value, one needs to have the free energy as a functional of correlation functions only. Such a functional can be derived as a Legendre transform of the free energy: $\Gamma=W-JG-K/2D-Lm$. The sources J,K and L have to be solved for G,D and m. The functional Γ is called a Baym-Kadanoff functional and its stationarity yields equations for zero source correlation functions. We present the functional without derivation:

$$\begin{aligned}\Gamma_{BK}[G,D,m]=&\operatorname{Tr}\ln G-\operatorname{Tr}(G_0^{-1}-G^{-1})G-\tfrac{1}{2}\operatorname{Tr}\ln D\\&+\tfrac{1}{2}\operatorname{Tr}D_0^{-1}D+\tfrac{1}{2}mD_0^{-1}m+\Phi[G,D,m].\end{aligned}\tag{D3}$$

G_0 and D_0 are free fields of the action, and the Φ functional is the sum of all two-particle irreducible graphs constructed from the original bare interaction vertices, from vertices generated by shifting the phonon field by m and from full correlation functions G and D.

The charge ordering instability can be studied by looking at the zero-frequency-momentum phonon propagator behavior: the propagator diverges in a charge-density-wave (CDW) transition. Alternatively one can study the transition from the ordered side, by observing the order parameter vanishing (m in our case). The two approaches should give consistent results. We will first show that this is indeed the case in the exact theory, then we explain how a similar approach can be applied in the EDMFT.

Let us introduce some compact notations we are going to use. o^a_α is a field operator of a kind at α space-time point. $a=G$ specifies an electron field operator and $a=D$ specifies a phonon field operator. $O^{ab}_{\alpha\beta,\gamma\delta}$ is a four-point function, which is a subset of all connected diagrams in the perturbative expansion of $\langle o^{a\dagger}_\alpha o^a_\beta o^{b\dagger}_\delta o^b_\gamma\rangle$; rules for selecting the subset of diagrams depend on a particular operator. Multiplication of two operators is defined by $[O^{(1)}O^{(2)}]_{\alpha\beta,\gamma\delta}=\Sigma_{\mu\nu}O^{(1)}_{\alpha\beta,\mu\nu}O^{(2)}_{\mu\nu,\gamma\delta}$. We introduce three four-point operators: (i) χ_0 includes all graphs which enter skeleton graphs without interaction vertices, (ii) Σ includes all one-particle irreducible with respect to a phonon line (1D) diagrams, and (iii) Γ includes all two-particle (2P) irreducible diagrams. In our case reducibility of $O_{\alpha\beta,\gamma\delta}$ is understood as disconnecting the $\alpha\beta$ part from the $\gamma\delta$ part. χ_0 is trivially expressed in terms of correlation functions: $\chi_0^{GD}=\chi_0^{DG}=0$, $\chi_{0\alpha\beta,\gamma\delta}^{GG}=G_{\alpha\gamma}G_{\beta\delta}$, and $\chi_{0\alpha\beta,\gamma\delta}^{DD}=D_{\alpha\gamma}D_{\beta\delta}+D_{\alpha\delta}D_{\beta\gamma}$.

We can write the following Dyson equations for the components of the Σ operator:

$$\begin{aligned}\Sigma^{GG}&=\chi_0^{GG}+\chi_0^{GG}\Gamma^{GG}\Sigma^{GG}+\chi_0^{GG}\Gamma^{GD}\Sigma^{DG},\\\Sigma^{GD}&=\chi_0^{GG}\Gamma^{GG}\Sigma^{GD}+\chi_0^{GG}\Gamma^{GD}\Sigma^{DD},\\\Sigma^{DG}&=\chi_0^{DD}\Gamma^{DD}\Sigma^{DG}+\chi_0^{DD}\Gamma^{DG}\Sigma^{GG},\\\Sigma^{DD}&=\chi_0^{DD}+\chi_0^{DD}\Gamma^{DD}\Sigma^{DD}+\chi_0^{DD}\Gamma^{DG}\Sigma^{GD}\end{aligned}\tag{D4}$$

or we could simply write

$$\Sigma=\chi_0+\chi_0\Gamma\Sigma.\tag{D5}$$

Solving for Σ we find $\Sigma=[\chi_0^{-1}-\Gamma]^{-1}=-(\partial^2\Gamma_{BK})^{-1}$. The second derivative $\partial^2\Gamma_{BK}$ is a 2×2 matrix defined by

$$(\partial^2\Gamma_{BK})_{ab}=\frac{\partial^2\Gamma_{BK}}{\partial C_a\partial C_b},\tag{D6}$$

where C is a two-component vector $C_G=G, C_D=D$.

The Σ matrix is related to the phonon self-energy Σ_{ph} in a simple way, as can be seen from the diagrammatic series in Fig. 16.

Σ comprises all four-legged 1P irreducible graphs, while Σ_{ph} comprises all two-legged 1P irreducible graphs. The 2P irreducible four-legged block is nothing but Γ. Two horizontal lines represent a couple of correlation functions of the same kind, GG or DD (we assume that a summation runs over each couple of horizontal lines), while 2P irreducible four-legged blocks are understood as 2×2 matrices. The first

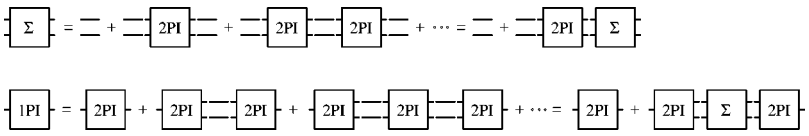

FIG. 16. Diagrammatic expansions for Σ and Σ_{ph}.

line is a diagrammatic analog of Eq. (D5). The second line provides connection between Σ and Σ_{ph}. That can be written as

$$\Sigma_{ph} = -\frac{\partial^2 \Phi}{\partial m \partial m} + \frac{\partial^2 \Phi}{\partial m \partial C_a} \Sigma^{ab} \frac{\partial^2 \Phi}{\partial C_b \partial m} \tag{D7}$$

or in a slightly different way,

$$\Sigma_{ph} = -\frac{\partial^2 \Phi}{\partial m \partial m} + \frac{\partial^2 \Gamma_{BK}}{\partial m \partial C} \left(\frac{\partial^2 \Gamma_{BK}}{\partial C \partial C'} \right)^{-1} \frac{\partial^2 \Gamma_{BK}}{\partial C' \partial m}. \tag{D8}$$

The condition for the CDW instability at wave vector q is $D_{0q}^{-1} - \Sigma_{ph} = 0$.

We will reproduce the above result studying the CDW transition from the ordered phase. Γ_{BK} is the free energy, so in the transition point

$$\frac{d^2 \Gamma_{BK}}{dm dm} = 0. \tag{D9}$$

From the way Γ_{BK} is constructed it follows $\partial \Gamma_{BK}/\partial C = 0$ and $d\Gamma_{BK}/dm = \partial \Gamma_{BK}/\partial m$. If we use $d(\partial \Gamma_{BK}/\partial C)/dm = 0$ and Eq. (D9) we find

$$\frac{\partial^2 \Gamma_{BK}}{\partial m \partial m} - \frac{\partial^2 \Gamma_{BK}}{\partial m \partial C} \left(\frac{\partial^2 \Gamma_{BK}}{\partial C \partial C'} \right)^{-1} \frac{\partial^2 \Gamma_{BK}}{\partial C' \partial m} = 0. \tag{D10}$$

This equation is identical to Eq. (D8), as it should be in exact theory. In the EDMFT approach we take the local approximation for the two-particle irreducible graphs. All 2P irreducible graphs in Γ_{BK} are contained by Φ. So the condition for m vanishing is still given by Eq. (D10) with Φ being local. Alternatively we can use Eq. (D5) where $\Gamma^{ab} = \partial^2 \Phi / \partial C_a \partial C_b$ is local, in which case these two methods are equivalent. Let us consider the second method, when the transition is approached from the disordered phase.

The local Γ^{ab} can be computed using the impurity action of EDMFT. For simplicity we consider electron-phonon interaction only, with the coupling $\lambda = 1$. Equations similar to Eq. (D4) can be written for the susceptibility $\chi^{ab} = \langle o^{a\dagger} o^a o^{b\dagger} o^b \rangle$. In short notation it reads:

$$\chi = \chi_0 + \chi_0 \tilde{\Gamma} \chi, \tag{D11}$$

where $\tilde{\Gamma}$ is different from Γ of Eq. (D5), because now it includes 1D reducible diagrams. The relation between $\tilde{\Gamma}$ and Γ is simple:

$$\tilde{\Gamma} = \Gamma + \hat{D}_0, \tag{D12}$$

where $\hat{D}_0$ is a 2×2 matrix, $\hat{D}_0^{GG} = D_0$, and $\hat{D}_0^{DG} = \hat{D}_0^{GD} = \hat{D}_0^{DD} = 0$. Using Eq. (D5), Eq. (D11), and Eq. (D12) we can express the self-energy Σ through the quantities which are directly computed from the impurity action:

$$\Sigma = ([\chi_{imp}]^{-1} - [\chi_{0imp}]^{-1} + \hat{D}_{0imp} + [\chi_0]^{-1})^{-1}, \tag{D13}$$

where $\chi_{imp}^{ab} = \langle o_a^\dagger o_a o_b^\dagger o_b \rangle_{imp}$, $\chi_{0imp}^{ab} = \delta_{ab} C_a^2$, and D_{0imp} is the Weiss field of the impurity action

$$\begin{aligned} S_{imp} = & \int d\tau d\tau' c_\sigma^\dagger(\tau) G_{0imp,\sigma}^{-1}(\tau - \tau') c_\sigma(\tau') \\ & + \frac{1}{2} \phi(\tau) D_{0imp}^{-1}(\tau - \tau') \phi(\tau') \\ & + \delta(\tau - \tau') \phi(\tau) c_\sigma^\dagger(\tau) c_\sigma(\tau). \end{aligned} \tag{D14}$$

The described method is exact in the limit $d \to \infty$. At finite d it yields a higher T_c than a naive local approximation $\Sigma_{ph} = \delta \Phi / \delta D$. Assuming $\Sigma_{ph} = \delta \Phi / \delta D$ would be equivalent to taking Γ_{BK} as being local in Eq. (D8), while the correct approach is to take a local approximation on the Φ functional only, not on the whole Baym-Kadanoff functional.

*Current address: Institute of Materials Science, University of Tsukuba, Tsukuba, Ibaraki, Japan.

[1] A. Georges, G. Kotliar, W. Krauth, and M.J. Rozenberg, Rev. Mod. Phys. **68**, 13 (1996), and references therein.
[2] S. Sachdev and J. Ye, Phys. Rev. Lett. **70**, 3339 (1993).
[3] H. Kajueter, Ph.D. thesis, Rutgers University, 1996; available at URL http://www.physics.rutgers.edu/~kotliar/thesis/kajueter.ps.gz
[4] Q. Si and J.L. Smith, Phys. Rev. Lett. **77**, 3391 (1996); Phys. Rev. B **61**, 5184 (2000).
[5] Q. Si, S. Rabello, K. Ingersent, and L. Smith, Nature (London) **413**, 804 (2001).
[6] R. Chitra and G. Kotliar, Phys. Rev. Lett. **84**, 3678 (2000).
[7] Y. Motome and G. Kotliar, Phys. Rev. B **62**, 12800 (2000).
[8] A. Georges, R. Siddharthan, and Serge S. Florens, Phys. Rev. Lett. **87**, 277203 (2001).
[9] R. Chitra and G. Kotliar, Phys. Rev. B **63**, 115110 (2001).
[10] H. Attias and Y. Alhassid, Nucl. Phys. A **625**, 565 (1997).
[11] J.K. Freericks, M. Jarrell, and D.J. Scalapino, Phys. Rev. B **48**, 6302 (1993).
[12] A.J. Millis, R. Mueller, and B.I. Shraiman, Phys. Rev. B **54**, 5389 (1996).
[13] C. Bloch and J.S. Langer, J. Math. Phys. **6**, 554 (1965)
[14] T. Holstein, Ann. Phys. (N.Y.) **8**, 325 (1959).
[15] J. Hubbard, Proc. R. Soc. London, Ser. A **281**, 401 (1964).
[16] M.J. Rozenberg, X.Y. Zhang, and G. Kotliar, Phys. Rev. Lett. **69**, 1236 (1992).
[17] A. Georges and G. Kotliar, Phys. Rev. B **45**, 6479 (1992).
[18] S. Lichtenstein, M. Katsnelson, and G. Kotliar, Phys. Rev. Lett. **87**, 067205 (2001).